Investigation of Optimal MCS and Subcarrier Spacing in MBSFN Systems

Kiril Kirev, Stefan Schwarz
Christian Doppler Laboratory for Dependable Wireless Connectivity for the Society in Motion
TU Wien, Institute of Telecommunications
Gusshausstrasse 25/389, A-1040 Vienna, Austria
Email: {kiril.kirev, stefan.schwarz}@tuwien.ac.at

***Abstract*—LTE Rel' 14 is the latest release in which enhancements to Multimedia Broadcast Multicast Services (MBMS) were introduced. Among the more prominent ones are the newly defined numerologies that allow for even smaller SubCarrier Spacing (SCS), the allowance for all resources in a subframe to be allocated to broadcasting services, dynamically allocate cells to dedicated broadcast transmission and new Modulation and Coding Scheme (MCS) values with support for up to 256 Quadrature Amplitude Modulation (QAM) modulation. These new numerologies define even longer Cyclic Prefixes to help combat multipath propagation effects with echoes with long delays, thus allowing for larger inter-cell distances. A natural consequence is the decrease in resource elements for user data and thus a decrease in maximum throughput. Another consideration is the increase in sensitivity towards Doppler spread with decreasing SCS, giving rise to a trade-off between user mobility and mitigating multipath echoes. In this paper we investigate combinations of MCS and SCS under a Single Frequency Network (SFN) transmission mode across the cell and towards the border in order to find the most resilient one under the assumption of user mobility and compare the performance to a multiple cell scenario with neighboring interferers.**

***Index Terms*—FeMBMS, LTE, MBSFN, SFN,**

I. Introduction

As trends in IP traffic tend to grow over the years, a surge in mobile multimedia traffic is also observed as user devices such as tablets and smartphones become technologically more advanced and convenient [1]. For delivery of parallel content, such as mobile TV, live streaming of specific events, or even mission-critical information, to multiple (multicast) or all (broadcast) clients, the most resource-efficient way is to utilize a Point-To-Multipoint (PTM) transmission over the same physical channel. Several standardization bodies have adopted technologies for broadcasting, such as Digital Video Broadcasting-Terrestrial (DVB-T/T2) [2], Multimedia Broadcast Multicast Services (MBMS) [3], Advanced Television Systems Committee (ATSC) [4], if we consider the purely terrestrial ones. In this paper our focus is on MBMS, however the obtained insights are also applicable to other Orthogonal Frequency Division Multiplexing (OFDM) based technologies, such as DVB-T2. MBMS was standardized and introduced by 3rd Generation Partnership Project (3GPP) in Rel' 6 for Universal Mobile Telecommunications System (UMTS) (in Rel' 9 for LTE) in order to optimize video traffic distribution. Since then there have been several changes, additions and enhancements to the standard, the current state-of-the-art version being Further enhanced Multimedia Broadcast Multicast Services (FeMBMS), introduced in Rel'14 LTE. As Rel'15 5G NR concentrated solely on unicast transmission, work on broadcasting has been frozen until a Working Group (WG) is freed, Rel'16 or Rel'17 [5]. Thus we focus solely on FeMBMS over LTE in this paper.

There are two defined transmission modes for broadcasting services in LTE besides the trivial approach of transmitting to each user over a different physical channel (Point-To-Point (PTP) transmission), namely Single Cell Point-To-Multipoint (SC-PTM) and Multicast-Broadcast Single-Frequency Network (MBSFN). The former one multiplexes unicast and broadcast traffic data over the same physical channel, namely the Physical Downlink Shared CHannel (PDSCH), only over a single cell. In contrast, multiple cells broadcast jointly in the latter mode which is the subject of interest in this paper and therefore we provide a brief description in the following subsection.

Notation: Bold lowercase letters ($\boldsymbol{a}$) denote vectors, bold uppercase ones denote matrices ($\boldsymbol{A}$). Conjugation is denoted by the superscript *, transposition by ^{T}, conjugate transposition by ^{H}, the Moore-Penrose pseudo inverse by †, the imaginary unit $\sqrt{-1}$ by j. Identity matrices of size B are denoted as $\boldsymbol{I}_B$. The operator $\operatorname{diag}(\boldsymbol{A})$ returns the main diagonal of $\boldsymbol{A}$ as a column vector.

A. MBSFN

In a typical cellular network architecture one would expect the worst reception conditions to be around the cell border. Degradation of the signal strength due to the physical distance, the presence of interfering signals from neighboring cells, where usually each cell transmits different data at different times, are the intuitive explanations. In MBSFN though each cell transmits the same signal, which can be exploited to combat interference effects. If all cells transmit in a synchronized manner, this destructive interference translates, in general, into useful signal power and improves reception quality. In practice however it would depend strongly on the number of transmitters, their relative positions, the relative delays between the received echoes and the propagation environment. As soon as the receiver detects a signal (a safe assumption here would be that the first arriving one would come from the nearest Base Station (BS)), it would synchronize to it, thus signals from other MBSFN BSs can be interpreted as multipath echoes of the first BS's signal. If these echoes arrive after the Cyclic Prefix (CP) duration of the underlying modulation and have sufficient power, the overall reception quality would degrade.

One of the main drawbacks of the SFN design is the static resource allocation which usually depends on the user with worst transmission conditions and thus limiting efficiency, as there is no Uplink channel in multicast mode and thus no feedback. In contrast, the SC-PTM mode could use the reported Channel State Information (CSI) of each link to adapt the Modulation and Coding Scheme (MCS) or SubCarrier Spacing (SCS) for the next allocated multicast slots.

B. Physical Layer Design

The resource allocation under SFN transmission mode follows the typical LTE downlink frame structure. Each radio frame has a temporal duration of $10\mathrm{ms}$ and comprises 10 subframes of length $1\mathrm{ms}$. Depending on the SCS a subframe is defined either as 2 slots of length $0.5\mathrm{ms}$ each or a single slot of length $1\mathrm{ms}$. The resource allocation is defined on this temporal granularity. Each slot consists of one Resource Block (RB) in the time.

The mapping between resource elements and physical transport channels is given by the RB. It is defined as N_{symb}^{DL} consecutive symbols in time and $N_{\mathrm{sc}}^{\mathrm{RB}}$ consecutive subcarriers in frequency. Together they comprise $N_{\mathrm{symb}}^{\mathrm{DL}} \times N_{\mathrm{sc}}^{\mathrm{RB}}$ resource elements, temporally equal to 1 slot or spectrally equal to $180\mathrm{kHz}$. Thus the effective transmission bandwidth is determined by the number of allocated RBs, the minimum number of which is 6. The time length of a slot is dependent on the SCS, denoted by F. Under FeMBMS transmission there are three defined values, namely $\{15, 7.5, 1.25\}\mathrm{kHz}$. For the former two, a slot duration is defined as 0.5ms and 1ms for the latter one. All corresponding parameters are listed in table I and are taken from [6]. For all SCS the CP comprises 20% of the total transmitted signal. It should also be noted at this point that the defined numerology calls for a denser pilot pattern (12.5% for $F = \{15, 7.5\}$kHz and 16.67% for $F = 1.25$kHz) in comparison to unicast numerologies (4.7%) and would further reduce the number of resource elements for data symbols, thus reducing the spectral efficiency. Furthermore, the denser pilot pattern for $F = 1.25\mathrm{kHz}$ means that this SCS will have fewer information bits but the same number of overall resource elements as the other two, leading to a higher code rate (i.e for $I_{\mathrm{MCS}} = 18, \mathrm{BW} = 1.4\mathrm{MHz}, R_{C,F=\{15,7.5\}\mathrm{kHz}} = 0.771, R_{C,F=1.25\mathrm{kHz}} = 0.809$) and higher SNR requirements for decoding correctly. Thus this SCS is inherently slightly negatively biased in comparison to the other two. We will not go into further details about the specific pilot patterns because channel estimation is not the scope of this paper. For more details the reader is referred to [7].

TABLE I: FeMBMS Numerology Options

F	$N_{\mathrm{slot}}^{\mathrm{SF}}$	$N_{\mathrm{sc}}^{\mathrm{RB}}$	$N_{\mathrm{symb}}^{\mathrm{DL}}$	T_{cp}	T_{symb}	ISD
15kHz	2	12	6	$16.7\mu s$	$66.7\mu s$	5km
7.5kHz	2	24	3	$33\mu s$	$133\mu s$	10km
1.25kHz	1	144	1	$200\mu s$	$800\mu s$	60km

$T_{symb} = \frac{1}{F}$, $T_{cp} = \frac{1\mathrm{ms}}{N_{\mathrm{slot}}^{\mathrm{SF}} \times \mathrm{N_{symb}}} - \mathrm{T}_{symb}$, ISD $\approx c_0 \times \mathrm{T_{cp}}$

F = Subcarrier Spacing, $\mathrm{N_{slot}^{SF}}$= Slots per Subframe, $N_{\mathrm{sc}}^{\mathrm{RB}}$ = Subcarriers per Resource Block, $N_{\mathrm{symb}}^{\mathrm{DL}}$ = OFDM Symbols per Slot, T_{cp}= Cyclic Prefix length, T_{cp}= Symbol Duration, ISD = Inter-Site Distance

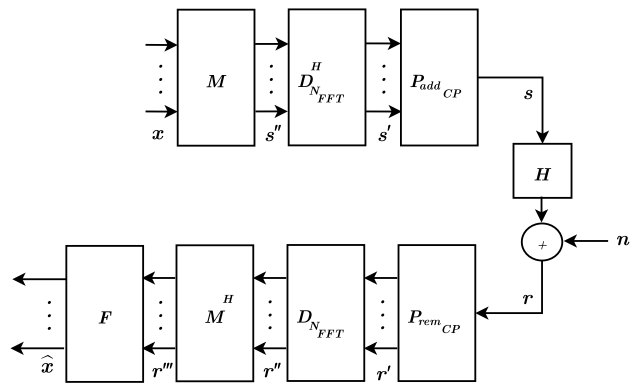

Fig. 1: Block Diagram of an OFDM system.

The motivation behind the smaller SCS is to help mitigate multipath propagation effects which lead to delayed and distorted versions of the transmit signal being superimposed at the receiver. LTE uses OFDM as a modulation waveform, where the signal is augmented with a partial copy of itself, i.e a CP, thus compensating for the spectral rotation caused by the delayed echoes [8]. As the logic goes, longer CP duration corresponds to a larger tolerable maximum excess delay τ_{max}, allowing larger Inter-Site Distance (ISD) in MBSFN. The defined MCS values can be found in [9], table 7.1.7.1-1 and table 7.1.7.1-1A.

II. Discrete-Time System Model

The block diagram of an LTE Downlink OFDM system is shown in fig. 1. Let $\boldsymbol{x} \in \mathbb{C}^{N_{SC} \times 1}$ be the input symbol vector:

$$\boldsymbol{x} = \begin{bmatrix} x_{i,0} & \dots & x_{i,l} & \dots & x_{i,N_{SC}-1} \end{bmatrix}^T, \tag{1}$$

where $x_{i,l}$ denotes the ith time symbol at subcarrier position l out of N_{SC}, chosen from a Quadrature Amplitude Modulation (QAM) alphabet. These complex symbols are then mapped onto the scheduled subcarriers by $\boldsymbol{M} \in \mathbb{R}^{N_{FFT} \times N_{SC}}$, where

N_{FFT} is the underlying Fast Fourier Transform (FFT) size. The mapped symbols are then fed into an OFDM modulator, which is described by the two matrices $\boldsymbol{D}^H_{N_{FFT}} \in \mathbb{C}^{N_{FFT}\times N_{FFT}}, \boldsymbol{P}_{add_{CP}} \in \mathbb{R}^{(N_{FFT}+N_{CP})\times N_{FFT}}$, N_{CP} being the CP length. The former matrix describes the Inverse Fast Fourier Transform (IFFT) and the latter one inserts the CP. The transmitted symbol can then be expressed as:

$$\boldsymbol{s} = \boldsymbol{P}_{add_{CP}} \boldsymbol{D}^H_{N_{FFT}} \boldsymbol{M}\boldsymbol{x} \in \mathbb{C}^{(N_{FFT}+N_{CP})\times 1}. \tag{2}$$

The transmitter side matrices are:

$$\boldsymbol{M} = \begin{bmatrix}\boldsymbol{0} & \boldsymbol{I}_{N_{SC}} & \boldsymbol{0}\end{bmatrix}^T, \tag{3}$$

$$\boldsymbol{D}^H_{N_{FFT}} = \left(\frac{\exp(-2\pi j)^{lk}}{\sqrt{N_{FFT}}}\right)^*_{l,k=0,\dots,N_{FFT}-1}, \tag{4}$$

$$\boldsymbol{P}_{add_{CP}} = \begin{bmatrix}\boldsymbol{0} & \boldsymbol{I}_{N_{CP}} \\ \multicolumn{2}{c}{\boldsymbol{I}_{N_{FFT}}}\end{bmatrix}. \tag{5}$$

The time domain convolution matrix is denoted by $\boldsymbol{H} \in \mathbb{C}^{(N_{FFT}+N_{CP})\times(N_{FFT}+N_{CP})}$ with elements $\boldsymbol{H}[i,m] = h[i-m,i]$, where $h[m,i]$ is the channel Impulse Response (IR) at time position i and lag m. The noise vector $\boldsymbol{n} \in \mathbb{C}^{(N_{FFT}+N_{CP})\times 1}$ is assumed to be zero mean, i.i.d Gaussian, $\boldsymbol{n} \sim \mathcal{CN}\big(\boldsymbol{0}, \sigma_n^2 \boldsymbol{I}_{(N_{FFT}+N_{CP})}\big)$. The received signal for an arbitrary user $\boldsymbol{r} \in \mathbb{C}^{(N_{FFT}+N_{CP})\times 1}$, where we omit the user index for brevity, is then:

$$\boldsymbol{r} = \boldsymbol{H}\boldsymbol{s} + \boldsymbol{n}. \tag{6}$$

The receiver chain then continues with removing the CP in the block $\boldsymbol{P}_{rem_{CP}} \in \mathbb{R}^{N_{FFT}\times(N_{FFT}+N_{CP})}$,

$$\boldsymbol{P}_{rem_{CP}} = \begin{bmatrix}\boldsymbol{0} & \boldsymbol{I}_{N_{FFT}}\end{bmatrix}. \tag{7}$$

Demodulating the OFDM signal by a FFT transform is done by $\boldsymbol{D}_{N_{FFT}}$ and then demapped by $\boldsymbol{M}^H$. It should be noted that generally $N_{FFT} \geq N_{SC}$ and in practice the FFT size is much greater. In that case the pseudo-inverse instead of the conjugate transpose should be taken, i.e $\boldsymbol{M}^H = \boldsymbol{M}^\dagger$. Lastly the equalizer $\boldsymbol{F} \in \mathbb{C}^{N_{SC}\times N_{SC}}$ is applied to negate the channel effects. Such full dimensional equalizer is computationally heavy. However, if the CP length is chosen such that the channel length does not surpass it and the Inter-Carrier Interference (ICI) is negligible, a diagonal (one-tap) equalizer is sufficient [10]. This leads to the expression of the symbol estimate $\hat{\boldsymbol{x}}$

$$\hat{\boldsymbol{x}} = \boldsymbol{F}\boldsymbol{M}^H \underbrace{\boldsymbol{D}_{N_{FFT}} \overbrace{\boldsymbol{P}_{rem_{CP}} \boldsymbol{H} \boldsymbol{P}_{add_{CP}}}^{\boldsymbol{H}'} \boldsymbol{D}^H_{N_{FFT}}}_{\boldsymbol{H}''} \boldsymbol{M}\boldsymbol{x} + \tilde{\boldsymbol{n}}, \tag{8}$$

where $\tilde{\boldsymbol{n}}$ is the transformed noise

$$\tilde{\boldsymbol{n}} = \boldsymbol{F}\boldsymbol{M}^H \boldsymbol{D}_{N_{FFT}} \boldsymbol{P}_{rem_{CP}} \boldsymbol{n}. \tag{9}$$

Up to now we have considered single-cell transmission only. To take into account multiple links from neighboring BSs, which would be the case in both MBSFN and Multiple Frequency Network (MFN) modes, we need to rewrite eq. (6). In the former case, all N_{BS} BSs transmit the same signal in a synchronized manner, thus the transmitter and receiver chain matrices are identical for each received signal and the only addition is to sum up the channel convolution matrices from all serving BSs, i.e

$$\boldsymbol{r}_{\text{MBSFN}} = \sum_{n_{BS}=1}^{N_{BS}} \boldsymbol{H}^{(n_{BS})} \boldsymbol{s} + \boldsymbol{n}, \tag{10}$$

where n_{BS} is the BS index. Depending on the propagation conditions, these additional terms might either act constructively by introducing delay diversity or destructively by effectively extending the channel duration with the additional echoes.

In case of MFN transmission, signals received from neighboring BSs act as interferers, the transmitter chain matrices are, in general but not necessarily, different for each received signal and eq. (6) has to be expanded by an extra cell interference term

$$\boldsymbol{r}_{\text{MFN}} = \boldsymbol{r} + \boldsymbol{n} + \sum_{n_{BS}=2}^{N_{BS}} \underbrace{\boldsymbol{H}^{(n_{BS})} \boldsymbol{P}^{(n_{BS})}_{add_{CP}} \boldsymbol{D}^H_{N_{FFT}} \boldsymbol{M}^{(n_{BS})} \boldsymbol{x}^{(n_{BS})}}_{\boldsymbol{r}_{\text{CI}}^{(n_{BS})}}, \tag{11}$$

where $\boldsymbol{r}_{\text{CI}}^{(n_{BS})}$ is the interference term caused by cell n_{BS} and acts solely destructively on the reception quality.

A. Model Augmentation

If the channel is time-invariant during transmission of the OFDM block and the CP is chosen accordingly ($N_{CP} > N_{Ch}$), then $\boldsymbol{H}_i$ would be of Toeplitz structure. If such is the case, adding and removing the CP turns $\boldsymbol{H}'$ into a circulant matrix, which then diagonalizes $\boldsymbol{H}''$ by the IFFT-FFT operations [11]. In case the CP does not cover the entire channel length, $\boldsymbol{H}'$ would no longer be circulant and $\boldsymbol{H}''$ would have nonzero off-diagonal elements which in turn would cause Inter-Symbol Interference (ISI) and ICI due to insufficient CP length. If the channel is further time-variant during an OFDM block, which is a valid assumption for mobile users, $\boldsymbol{H}$ would also no longer be of Toeplitz structure. Then the impact of the previous OFDM block on the current one has to be considered. We assume the receiver evaluation frame captures only a single precursor frame in order to exclude the impact of the postcursor frame. The authors in [12] derive a time-variant representation of the work in [13] that represents the received signal $\boldsymbol{r}'$ after CP removal as

$$\boldsymbol{r}' = \underbrace{\boldsymbol{H}_{ave}\boldsymbol{s}'}_{\boldsymbol{r}_1} + \underbrace{\boldsymbol{H}_{var}\boldsymbol{s}'}_{\boldsymbol{r}_2} + \underbrace{\boldsymbol{B}\tilde{\boldsymbol{s}}'}_{\boldsymbol{r}_3} - \underbrace{\boldsymbol{A}\boldsymbol{s}'}_{\boldsymbol{r}_4} + \boldsymbol{n}, \tag{12}$$

where $\boldsymbol{r}_1$ is the desired term without ISI & ICI, $\boldsymbol{r}_2$ is the ICI component due to channel variations, $\boldsymbol{r}_3$ is the ISI component from the previous frame and $\boldsymbol{r}_4$ is the ICI component from the current frame. The channel matrices $\boldsymbol{H}_{ave}$, $\boldsymbol{H}_{var}$, $\boldsymbol{A}$ and $\boldsymbol{B}$ incorporate the CP addition and removal matrices in them, in the same manner as $\boldsymbol{H}'$ in eq. (8), and their definitions can be found in [12]. Lastly $\boldsymbol{s}'$ and $\tilde{\boldsymbol{s}}'$ represent the current and previous modulated symbols, respectively, before CP addition. We could thus decompose the received signal into useful part, $\boldsymbol{r}_1$, and distortion parts, $\boldsymbol{r}_2, \boldsymbol{r}_3, \boldsymbol{r}_4, \tilde{\boldsymbol{n}}$. The useful symbol power $\boldsymbol{\rho}^2_{\boldsymbol{r}_1} = \operatorname{diag}\left(\mathbb{E}\{\boldsymbol{r_1}\boldsymbol{r_1}^H\}\right)$ for white data can be calculated as follows:

$$\begin{aligned}\boldsymbol{\rho}^2_{\boldsymbol{r}_1} =& \operatorname{diag}\Big(\boldsymbol{F}\boldsymbol{M}^H\boldsymbol{D}_{N_{FFT}}\boldsymbol{H}_{ave}\boldsymbol{D}^H_{N_{FFT}}\boldsymbol{M}\mathbb{E}\{\boldsymbol{x}\boldsymbol{x}^H\} \\ & \boldsymbol{M}^H\boldsymbol{D}_{N_{FFT}}\boldsymbol{H}^H_{ave}\boldsymbol{D}^H_{N_{FFT}}\boldsymbol{M}\boldsymbol{F}^H\Big) = \\ =& \sigma_x^2\operatorname{diag}\Big(\boldsymbol{F}\boldsymbol{M}^H\boldsymbol{H}''_{ave}\boldsymbol{M}\big(\boldsymbol{F}\boldsymbol{M}^H\boldsymbol{H}''_{ave}\boldsymbol{M}\big)^H\Big),\end{aligned} \tag{13}$$

where in a slight abuse of notation, $\boldsymbol{H}''$ represents the FFT-IFFT operations on a matrix, i.e $\boldsymbol{H}'' = \boldsymbol{D}_{N_{FFT}}\boldsymbol{H}\boldsymbol{D}^H_{N_{FFT}}$. Analogously we represent the power contribution of the various interference and noise terms post equalization as:

$$\boldsymbol{\rho}^2_{\boldsymbol{r}_2} = \sigma_x^2\operatorname{diag}\Big(\boldsymbol{F}\boldsymbol{M}^H\boldsymbol{H}''_{var}\boldsymbol{M}\big(\boldsymbol{F}\boldsymbol{M}^H\boldsymbol{H}''_{var}\boldsymbol{M}\big)^H\Big), \tag{14}$$

$$\boldsymbol{\rho}^2_{\boldsymbol{r}_3+\boldsymbol{r}_4} = 2\sigma_x^2\operatorname{diag}\Big(\boldsymbol{F}\boldsymbol{M}^H\boldsymbol{B}''\boldsymbol{M}\big(\boldsymbol{F}\boldsymbol{M}^H\boldsymbol{B}''\boldsymbol{M}\big)^H\Big), \tag{15}$$

$$\boldsymbol{\rho}^2_{\tilde{\boldsymbol{n}}} = \sigma_n^2\operatorname{diag}\Big(\boldsymbol{F}\boldsymbol{F}^H\Big), \tag{16}$$

where we utilize the results in [14] that the ISI & ICI terms due to insufficient CP have the same Power Spectral Density (PSD). Since $\boldsymbol{A}$ is a permuted version of $\boldsymbol{B}$, it does not matter which channel matrix is used for calculating eq. (16). Finally we can express the Signal-to-Interference plus Noise Ratio (SINR) per subcarrier k as

$$\mathrm{SINR}\,[\mathrm{k}] = \frac{\boldsymbol{\rho}^2_{\boldsymbol{r}_1}[k]}{\boldsymbol{\rho}^2_{\boldsymbol{r}_2}[k] + \boldsymbol{\rho}^2_{\boldsymbol{r}_3+\boldsymbol{r}_4}[k] + \boldsymbol{\rho}^2_{\tilde{\boldsymbol{n}}}[k]}. \tag{17}$$

This expression is valid both for single-signal reception and for MBSFN transmission mode as the extra signal contributions are incorporated additively in the convolution matrices. For MFN transmissions, the inter-cell interference power contributions,

$$\begin{aligned}\boldsymbol{\rho}^2_{\boldsymbol{r}_{\mathrm{CI}}^{(n_{BS})}} =& \sigma^2_{x^{(n_{BS})}}\operatorname{diag}\Big(\boldsymbol{G}^{(n_{BS})}\big(\boldsymbol{G}^{(n_{BS})}\big)^H\Big), \\ \boldsymbol{G}^{(n_{BS})} =& \boldsymbol{F}\boldsymbol{M}^H\boldsymbol{D}_{N_{FFT}}\boldsymbol{P}_{rem_{CP}}\boldsymbol{H}^{(n_{BS})}\boldsymbol{P}^{(n_{BS})}_{add_{CP}}\boldsymbol{D}^H_{N_{FFT}}\boldsymbol{M}^{(n_{BS})},\end{aligned} \tag{18}$$

need to be accounted for and the SINR equation becomes

$$\mathrm{SINR}\,[\mathrm{k}] = \frac{\boldsymbol{\rho}^2_{\boldsymbol{r}_1}[k]}{\boldsymbol{\rho}^2_{\boldsymbol{r}_2}[k]+\boldsymbol{\rho}^2_{\boldsymbol{r}_3+\boldsymbol{r}_4}[k]+\boldsymbol{\rho}^2_{\tilde{\boldsymbol{n}}}[k]+\sum_{n_{BS}=2}^{N_{BS}}\boldsymbol{\rho}^2_{\boldsymbol{r}_{\mathrm{CI}}^{(n_{BS})}}[k]}. \tag{19}$$

B. Pathloss

In order to relate distances to signal power, a pathloss model needs to be applied. For the purposes of this paper we have chosen the Okumura-Hata model [15]. It is an empirical model based on extensive measurements in Tokyo in the '60s made by Okumura and then extended by Hata in the '80s and still widely used today. The resulting pathloss is directly dependent on transmitter and receiver heights (denoted h_b and h_m, respectively), the distance between them and on the carrier frequency f_c. Environment-dependent factors, $a\left(h_m\right)$ and C are then introduced to account for propagation conditions. The mathematical expression is then:

$$\mathrm{PL[dB]} = \mathrm{A} + \mathrm{B}\log_{10}(d) + \mathrm{C}, \tag{20}$$

$$\begin{aligned}\mathrm{A} =& 69.55 + 26.16\log_{10}(f_c) - 13.82\log_{10}(h_b) \\ & - a\left(h_m\right),\end{aligned} \tag{21}$$

$$\mathrm{B} = 44.9 - 6.55\log_{10}(h_b). \tag{22}$$

We consider a medium-sized city, thus the environment factors are given as [16]:

$$\begin{aligned}a\left(h_m\right) =& \left(1.1\log_{10}(f_c) - 0.7\right) \\ & - \big(1.56\log_{10}(f_c) - 0.8\big),\end{aligned} \tag{23}$$

$$C = 0. \tag{24}$$

III. Simulation Setup

We consider two homogeneous neighboring cell sites and compare the MBSFN transmission mode to one where signals from a neighboring cell are considered as interference, and also to the case where the neighboring cell is switched off, thus no interference is observed. The former case could be seen as a simplified SC-PTM transmission without interference mitigation strategies employed, such as power and subcarrier allocation, frequency reuse, etcetera. Therefore this transmission scenario is referred to as SC-PTM. The scenario with switched off neighboring cell is an idealistic case and serves as baseline for the choice of MCS index, as such spatially isolated cell without immediate neighbors does not represent a common scenario in practice. It will be referred to as single-cell transmission.

The simulations were carried out on the Vienna 5G Link Level Simulator [17]. We place the receiver on a straight line between the centers of both cells and evaluate the performance across the main cell, directly towards the cell border with the neighbor cell. The relevant simulation parameters are listed in table II. We assume two cell dimensions, described by their ISDs and transmit powers. The first cell has a radius $\mathrm{R} = \mathrm{ISD}/2$ of 5km and Effective Isotropic Radiated Power (EIRP) of $53\mathrm{dBm}$. The latter parameter can be interpreted as a combination of transmit power $\mathrm{P}_{\mathrm{tx},1} = 43\mathrm{dBm} \triangleq 20\mathrm{W}$ and antenna Gain $G_{tx} = 10\mathrm{dBi}$, which are values in the range of a standard macro cell deployment [18]. In the second scenario we double the cell radius and transmit power ($\mathrm{R}_2 = 10\mathrm{km}$ and $\mathrm{P}_{\mathrm{tx},1} = 46\mathrm{dBm} \triangleq 40\mathrm{W}$, respectively) and keep the same antenna gain. We are interested in mobile user scenarios and assume walking $v = 5\mathrm{km/h}$ and inner-city driving $v = 50\mathrm{km/h}$ velocities. Static cases and higher velocities are outside of the scope of this publication.

IV. Simulation Results

The procedure for choosing the optimal MCS index for the considered scenarios is the following: We compute the achievable throughput at the cell border for the case where a single cell is active and there are no interferers, i.e single-cell transmission, for both ISDs and both velocities v. The chosen SCS is $15\mathrm{kHz}$ as it is most susceptible to performance degradation due to its shorter CP length. The calculated

TABLE II: Simulation Parameters

Channel model:	Rayleigh Fading
Power Delay Profile @5km/h:	Pedastrian B [19]
Power Delay Profile @50km/h:	Vehicular B [19]
Doppler Model:	Jakes
Rx Movement Speed:	$\{5, 50\}$km/h
Monte Carlo repetitions:	1000
Channel Coding:	Turbo
System bandwidth:	1.4MHz
Guard Band:	320kHz
Equalizer:	Zero Forcing
ISD:	$\{10, 20\}$km
EIRP:	$\{53, 56\}$dBm
Tx height:	30m
Rx height:	1.5m
Carrier Frequency:	800MHz
Chann. Estimation:	Perfect Channel
Sampling Frequency:	1.92MHz

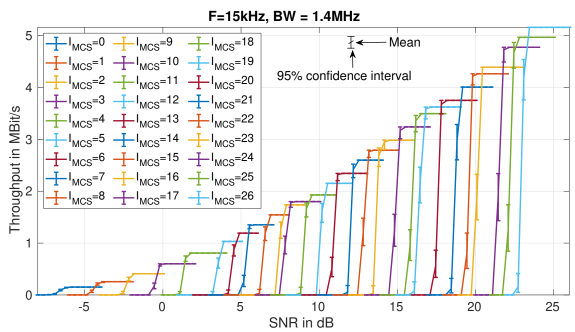

Fig. 2: Achievable throughput, AWGN

throughput value for each MCS index is then compared to its respective maximum achievable value under Additive White Gaussian Noise (AWGN) conditions, which could be read out from fig. 2. The index with the lowest degradation in throughput is then taken for the simulations.

For $\mathrm{R} = 5\mathrm{km}$ and $v = 5\mathrm{km/h}$, MCS index 12 achieves the highest throughput of all indices ($1.956\mathrm{MBit/s}$). Compared to the maximum achievable value under AWGN ($2.152\mathrm{MBit/s}$), the performance degradation is 9.11%. For the same same cell radius R and $v = 50\mathrm{km/h}$, MCS index 12 again has the highest calculated throughput $1.745\mathrm{Bit/s}$, which results in 18.91% degradation. Therefore $I_{\mathrm{MCS}} = 12$ is the index of choice for smaller cell scenario.

For $\mathrm{R} = 10\mathrm{km}$ and $v = 5\mathrm{km/h}$, the highest calculated throughput belongs to $I_{\mathrm{MCS}} = 8$ ($1.053\mathrm{MBit/s}$). With ($1.544\mathrm{MBit/s}$) being the maximum achievable value for this MCS, the performance degradation calculates to 31.8%. Lastly, for the same R and $v = 50\mathrm{km/h}$, $I_{\mathrm{MCS}} = 7$ has the highest calculated throughput at the cell border ($1.03\mathrm{MBit/s}$). The maximum achievable value for this MCS index is ($1.352\mathrm{MBit/s}$) and therefore the degradation is calculated to be 23.78%.

With the chosen MCS values for each cell scenario and user velocity, simulation results for all three transmission modes and SCS are shown in figs. 3 to 6. The former two figures

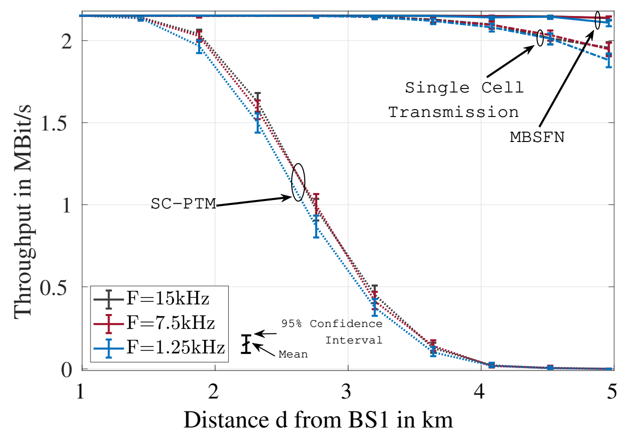

Fig. 3: $R = 5\mathrm{km}$, $v_{\mathrm{UE}} = 5\mathrm{km/h}$, $I_{\mathrm{MCS}} = 12$

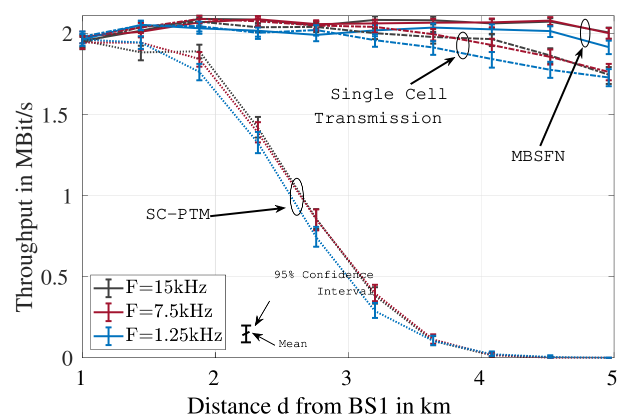

Fig. 4: $R = 5\mathrm{km}$, $v_{\mathrm{UE}} = 50\mathrm{km/h}$, $I_{\mathrm{MCS}} = 12$

represent the scenario where the two BSs are separated by an ISD of $10\mathrm{km}$. The receiver is assumed to be moving along a line towards the neighboring cell, starting $1\mathrm{km}$ away from the first BS, which is taken as the main one. This means that the user will synchronize to it, whereas the transmit signal of the other one will be received with a delay $\tau = \frac{d_n - d_m}{c_0}$, where d_m and d_n are the user distances from the main and neighboring BS, respectively. In both scenarios and for both velocities, SC-PTM transmission gets buried under inter-cell-interference for small distances d and is obviously the primary performance-limiting factor. Excluding it, both other transmissions perform relatively consistent along the path, with MBSFN having a slight gain near the cell border. It should be noted that the chosen scenarios represent metropolitan areas where interference is the main limiting factor. For a clearer highlight of the SFN gain a scenario closer to traditional terrestrial radio broadcast towers is advised. As for the choice of the SCS, for $F = 1.25\mathrm{kHz}$ a performance loss is observed due to the inherently higher coding rate of this numerology and the Doppler frequency. The other two SCS perform similar under the chosen conditions.

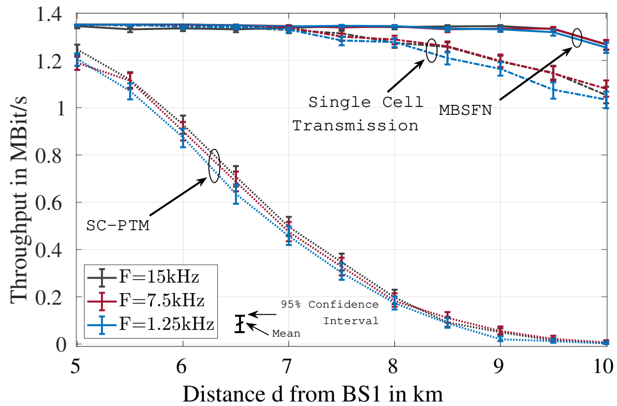

Fig. 5: $R = 10\text{km}$, $v_{\text{UE}} = 5\text{km/h}$, $I_{\text{MCS}} = 8$

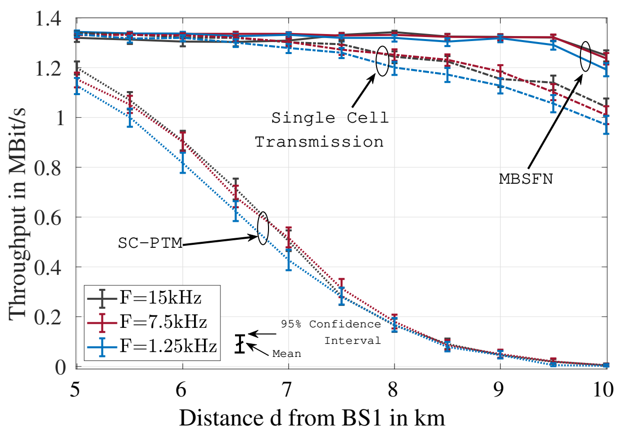

Fig. 6: $R = 10\text{km}$, $v_{\text{UE}} = 50\text{km/h}$, $I_{\text{MCS}} = 7$

V. Conclusion

In this paper we provide a general description of LTE's MBSFN service. A linear transmission model was derived which could serve for further performance evaluation, depending on the use case. Under this framework the individual performance deteriorating factors can be calculated and the optimal choice of MCS and SCS could be made accordingly. We present two simulation scenarios and we consider slowly moving users such as pedestrians and urban commuters. We compare MBSFN transmission to a two-cell scenario with and without neighboring interferers.

VI. Acknowledgements

This work has been funded by the Christian Doppler Laboratory for Dependable Wireless Connectivity for the Society in Motion. The financial support by the Austrian Federal Ministry for Digital and Economic Affairs and the National Foundation for Research, Technology and Development is gratefully acknowledged.

References

[1] Cisco Visual Networking Index. "Global mobile data traffic forecast update, 20162021 white paper." Cisco: San Jose, CA, USA (2017).
[2] Eizmendi, Inaki, et al. "DVB-T2: The second generation of terrestrial digital video broadcasting system." IEEE transactions on broadcasting 60.2 (2014): 258-271.
[3] Lecompte, David, and Frdric Gabin. "Evolved multimedia broadcast/multicast service (eMBMS) in LTE-advanced: overview and Rel-11 enhancements." IEEE Communications Magazine 50.11 (2012): 68-74.
[4] Fay, Luke, et al. "An overview of the ATSC 3.0 physical layer specification." IEEE Transactions on Broadcasting 62.1 (2016): 159-171.
[5] Forward Compatibility Consideration for ECP Design and NR-MBMS,document R1-1712879, 3GPP, Sophia Antipolis, France, Aug. 2017
[6] 3rd Generation Partnership Project (3GPP); Technical Specification Group Radio Access Network; Evolved Universal Terrestrial Radio Access (E-UTRA); Physical channels and modulation. TS 36.211 (Release 14).
[7] Van De Beek, J-J., et al. "On channel estimation in OFDM systems." 1995 IEEE 45th Vehicular Technology Conference. Countdown to the Wireless Twenty-First Century. Vol. 2. IEEE, 1995.
[8] Peled, Abraham, and Antonio Ruiz. "Frequency domain data transmission using reduced computational complexity algorithms." ICASSP'80. IEEE International Conference on Acoustics, Speech, and Signal Processing. Vol. 5. IEEE, 1980.
[9] 3rd Generation Partnership Project (3GPP); Technical Specification Group Radio Access Network; Evolved Universal Terrestrial Radio Access (E-UTRA); Physical layer procedures. TS 36.213 (Release 14)
[10] Hirosaki, Botaro. "An analysis of automatic equalizers for orthogonally multiplexed QAM systems." IEEE Transactions on Communications 28.1 (1980): 73-83.
[11] Zchmann, Erich, et al. "Limited feedback in OFDM systems for combating ISI/ICI caused by insufficient cyclic prefix length." 2014 48th Asilomar Conference on Signals, Systems and Computers. IEEE, 2014.
[12] Chen, Shaoping, and Cuitao Zhu. "ICI and ISI analysis and mitigation for OFDM systems with insufficient cyclic prefix in time-varying channels." IEEE Transactions on Consumer Electronics 50.1 (2004): 78-83.
[13] Zhu, Jie, Wee Ser, and A. Nehorai. "Channel equalization for DMT with insufficient cyclic prefix." Conference Record of the Thirty-Fourth Asilomar Conference on Signals, Systems and Computers (Cat. No. 00CH37154). Vol. 2. IEEE, 2000.
[14] Henkel, Werner, et al. "The cyclic prefix of OFDM/DMT-an analysis." 2002 International Zurich Seminar on Broadband Communications Access-Transmission-Networking (Cat. No. 02TH8599). IEEE, 2002.
[15] Hata, Masaharu. "Empirical formula for propagation loss in land mobile radio services." IEEE transactions on Vehicular Technology 29.3 (1980): 317-325.
[16] Molisch, Andreas F. Wireless Communications. Vol. 34. John Wiley & Sons, 2012, ch. 7.A.
[17] Pratschner, Stefan, et al. "Versatile mobile communications simulation: The Vienna 5G link level simulator." EURASIP Journal on Wireless Communications and Networking 2018.1 (2018): 226.
[18] Arnold, Oliver, et al. "Power consumption modeling of different base station types in heterogeneous cellular networks." 2010 Future Network & Mobile Summit. IEEE, 2010.
[19] 3rd Generation Partnership Project (3GPP). Technical Specication Group Radio Access Network; High Speed Downlink Packet Access: UE Radio Transmission and Reception. TR 25.890. 3rd Generation Partnership Project (3GPP), May 2002.